IEEE Access
Multidisciplinary | Rapid Review | Open Access Journal

Received May 20, 2019, accepted June 11, 2019, date of publication June 17, 2019, date of current version July 1, 2019.

Digital Object Identifier 10.1109/ACCESS.2019.2923581

Validation of Potential Effects on Human Health of in Vivo Experimental Models Studied in Rats Exposed to Sub-Thermal Radiofrequency. Possible Health Risks Due to the Interaction of Electromagnetic Pollution and Environmental Particles

AARON A. SALAS-SÁNCHEZ[1], ALBERTO LÓPEZ-FURELOS[2], J. ANTONIO RODRíGUEZ-GONZÁLEZ[1], (Senior Member, IEEE), FRANCISCO J. ARES-PENA[1], (Fellow, IEEE), AND M. ELENA LÓPEZ-MARTíN[2]

[1]Department of Applied Physics, University of Santiago de Compostela, Santiago de Compostela 15782, Spain
[2]Department of Morphological Sciences, University of Santiago de Compostela, Santiago de Compostela 15782, Spain

Corresponding author: Francisco J. Ares-Pena (francisco.ares@usc.es)

This work was supported in part by the FEDER/Ministerio de Ciencia, Innovación y Universidades-Agencia Estatal de Investigación under Project TEC2017-86110-R.

ABSTRACT Studies are based on the exposure of Sprague–Dawley rats (250 male and 250 female rats) to electromagnetic fields (EMF) at different frequencies in standing and travelling wave chambers. Values of specific absorption rate (SAR) for all of these experiments were obtained from commercially available FDTD-based simulation software based on numerical phantom animals. An experimental radiation system was developed with a standing-wave cavity which keeps electromagnetic parameters constant while facilitating stress-free exposure of animals to non-thermal radiation. This makes it possible to directly measure the power absorbed by the animal and determine whole-body mean SAR according to weight. All studies using this setup were performed with global system for mobile communication (GSM) radiation at 900 MHz. The simple picrotoxin model made allow to identify morphological signs of neurotoxicity in rat brain tissue. Experiments involving travelling waves were done in a commercial Gigahertz Transverse ElectroMagnetic (GTEM) chamber connected to one or two vector signal generators (to carry single or multiple EMF exposure frequencies). In the diathermy model, rat thyroid and thymus exposed to 2.45 GHz radiation showed visible morphological and immune effects. Cellular stress in the cerebral cortex, the cerebellum or both seems to be more associated with the type of signal than with additive effects of combined frequencies. Finally, some hypothesis related with the future models about the ElectroMagnetic (EM) pollution are established. In an urban environmental that combines the electromagnetic and chemical pollution of environmental particles, cortical excitability, inflammatory response, and cell injury can be modified.

INDEX TERMS Bioelectromagnetic effects, electromagnetic radiation effects, specific absorption rate.

I. INTRODUCTION

ElectroMagnetic Fields (EMF) are pervasive in everyday life. Antennas, including GSM (Global System for Mobile Communication) antennas for cell phones in towns and cities expose most of the human population to radiation at multiple frequencies, especially RadioFrequency (RF). Copious research in the last decade has described changes in the biological parameters of living organisms after contact

The associate editor coordinating the review of this manuscript and approving it for publication was Huapeng Zhao.

This work is licensed under a Creative Commons Attribution 3.0 License. For more information, see http://creativecommons.org/licenses/by/3.0/

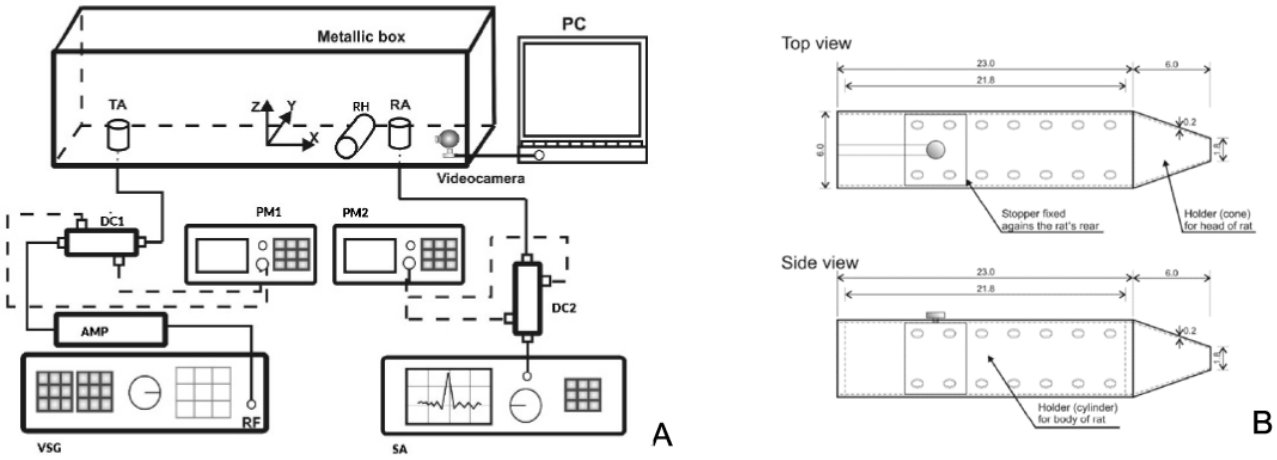

FIGURE 1. A) Sketch of the Experimental System I. Vector Signal Generator (VSG), Spectrum Analyser (SA) and Power Meters (PM1, PM2) from Agilent (Models E4438C, E4407B and E4418B, respectively), Linear Power Amplifier (AMP) from Amplifier Research (Model AR 15S1G3), and Directional Couplers (DC1, DC2) from Narda (Model 3282B-30). TA, Transmitting Antenna; RA, Receiving Antenna. Coordinates originate at the center of the chamber floor. B) Geometrical dimensions of the methacrylate holder (RH).

with EMF. Some segments of the population may be more vulnerable to potentially adverse effects stemming from work exposure or individual susceptibility. Relevant epidemiological and experimental studies have attempted to evaluate EMF exposure and its effects on cancer risk [1], the nervous system [2], hematology [3], metabolism and the endocrine system [4] and the human population at large or specific groups that may incur greater risk due to more direct exposure.

While many experimental studies have looked at how non-ionizing radiation affects human health or animal models, the methodology used critically influences the objectivity of the results. The experimental radiation system must be selected with great care when doing laboratory research with biological models and animals in vivo. Specifically, the electromagnetic test chamber must provide a controlled experimental environment that will facilitate subsequent analysis of the electromagnetic parameters and dosimetry calculations.

To further our understanding of the effects of non-ionizing radiation in living organisms at the Bioelectromagnetics Laboratory of the University of Santiago de Compostela, we tested several rat animal models in experiments involving controlled exposure to radio frequencies that are habitually used for wireless devices, Wi-Fi or rehabilitation therapy [5], [6]. By administering a subconvulsive dose of picrotoxin (GABA-A receptor antagonist), we developed a neurological rat model [7] to look at the effects of radiation on preconvulsive brain function. We also examined tissue morphology using a diathermic model that exposed the left front leg of a female rat to maximum subthermal radiation in order to assess the impact on cellular stress [8]. Recently, we created a lifelike scenario in the laboratory to explore harmful effects stemming from simultaneous exposure to two combined radiofrequencies [9].

II. DESCRIPTION OF EXPERIMENTAL RADIATION SYSTEMS

A. EXPERIMENTAL SYSTEM I: STANDING WAVE CAVITY

In this experimental system, designed by the Radiating Systems Group at University of Santiago de Compostela, the animal is put inside a methacrylate holder (RH) and positioned in the area of maximum radiation inside a metal cavity. The RH is large enough to minimize stress to the animals except for the head which because it cannot move imparts some stress. There is also a transmitting antenna (TA), a receiving antenna (RA) and a video camera within the cavity (see Fig. 1.A).

Signal frequency, amplitude and modulation were ascertained by using a generator that was attached to an amplifier. A directional coupler then carried the amplified signal to the transmitting antenna inside the cavity, where radiation occurred. A pure 900 MHz sinusoidal signal was used for the experiments discussed here.

The receiving antenna (RA) inside the cavity was connected to an external spectrum analyzer. This served to monitor and verify field stability, as well as to ensure the absence of spurious signals.

The directional couplers, sensors and power meters composing the subsystem make it possible to determine the power absorbed by the animal. This is calculated as the difference in power absorbed by the system with and without the rat inside the box.

To determine optimal RH placement (see dimensions in Fig. 1.B), we had to first quantify field distribution within the radiation area. We used commercially available SPEAG SEMCAD Finite-Difference Time-Domain (FDTD) software to model the metal cage, removing the RA and the RH and keeping only the TA inside. For the simulation, the TA was modelled as a $\lambda/4$ monopole. A perfect electric conductor (PEC) corresponding to the metal box limited the radiation region, as shown in Fig. 1.A. The computational

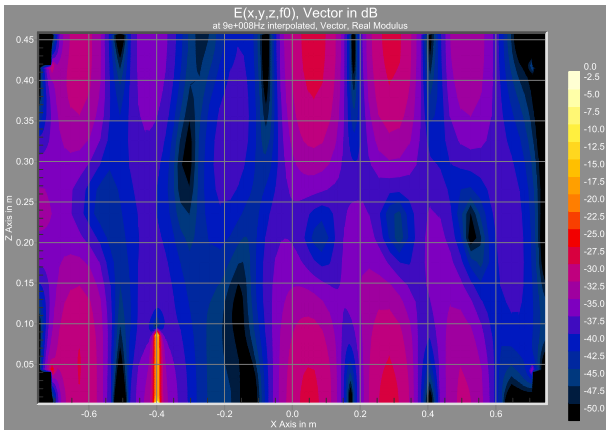

FIGURE 2. |E| field distribution within the metallic cavity with only the transmitting antenna in place. The distribution corresponds to section Y=0 of Fig. 1.A, while Z and X correspond to the axes shown in Fig. 1.A.

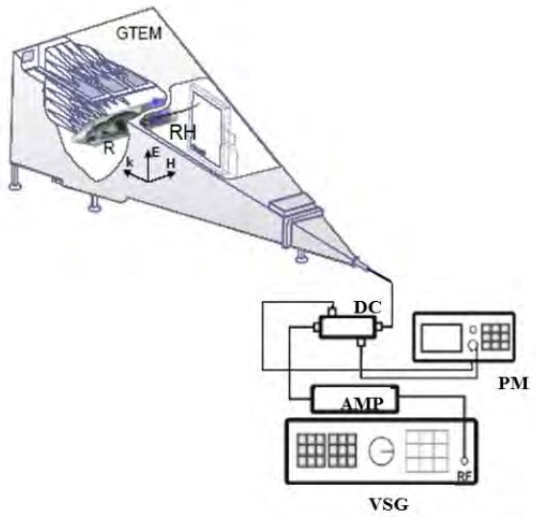

FIGURE 3. Diagram of Experimental System II. GTEM cell (Schaffner 250 irradiation chamber); VSG: Vector Signal Generator (Agilent E4438C: 250 kHz-4 GHz); AMP: Amplifier (Research Amplifier 15S1G3: 0.8–3 GHz); DC: Directional Coupler (NARDA 3282B-30: 800-4000 MHz); PM: Power Meter (Agilent E4418B); RH: Rat Holder.

domain was filled with 0.5 million 3D cells and steady-state was achieved after 400 sinusoidal periods. Field distribution $|E|$ was calculated within the radiation region and is shown in Fig. 2. Local maxima and minima in the resulting field were very helpful for indicating the most suitable placement of the RH and the RA.

Once the final positions had been determined, it was easy to calculate the power available in the system, the power delivered to the receiving antenna and the power dissipated in the system.

B. EXPERIMENTAL SYSTEM II: TRAVELLING WAVE CAVITY AT SINGLE FREQUENCY

In this experimental set-up, the Vector Signal Generator (VSG) sent a pure sinusoidal signal of 2.45 GHz to the amplifier at the specified power level during radiation. The amplifier was connected to the directional coupler (DC) and output passed into the GTEM radiation chamber. This is a Schaffner 250 Gigahertz Transverse ElectroMagnetic chamber of 1.25m $\times$ 0.65m $\times$ 0.45m, where the rat (R) was immobilized in the holder (RH) and positioned in the zone of maximum field uniformity in such a way that the left front leg of the animal would receive maximum radiation. The animal was then irradiated. The DC measured incident power values by means of the spectrum analyzer and obtained reflected power values from the power meter (PM) (see Fig. 3).

C. EXPERIMENTAL SYSTEM III: TRAVELLING WAVE CAVITY, MULTIPLE FREQUENCIES

In Experimental System III, each of the two vector signal generators (VSG1 and VSG2) generates a pure sinusoidal signal of 900 MHz and 2.45 GHz, respectively, at the desired power level during radiation. Both generators are hooked up to a signal mixer (SM) which more concretely acts as a power combiner. This signal is transmitted to the amplifier (AMP), as shown in Fig. 4.A.

We used MATLAB scientific software to simulate the 900 MHz and 2.45 GHz pure signals separately and the sum of both signals (900 MHz + 2.45 GHz), as depicted in Fig. 4.B. In the laboratory, the simulated combined signal was also validated at lower frequencies using the Agilent Infinium (600 MHz) oscilloscope to visualize the combined output signal.

Once amplified, the signal entered the directional coupler (DC) and passed directly into the GTEM radiation chamber, where the rat (R) was immobilized in the holder (RH) and positioned in the zone of maximum field uniformity in such a way that the left front leg of the animal would receive maximum radiation. The animal was then irradiated. The DC enabled measurement of incident power by means of the Power Meter (PM), making it possible to verify the specified input power to the system. Using the spectrum analyzer (SA), reflected power values could also be measured and monitored, and the spectral purity of the sinusoid signal used in the experiment could be verified.

As the field impinged on R in the direction k, with vectors E and H positioned perpendicular and parallel to the main axis of the animal, respectively, the left front region of R received maximum field amplitude. The isotropic probe (IP) measured the field and determined its peak value, using the desired input signal values when the rat was not in the chamber. In this way, we quantified how the chamber behaves in the measurement zone. Later, we will use two plane wave fronts to reproduce the data obtained with the probe and provide a more objective simulation of the GTEM chamber.

III. ANIMALS, AND PROTOCOLS.

All the experimental animals were male or female Sprague-Dawley rats with an approximate weight of 200-250 gr. They were previously treated, in standard conditions (12/12 h of light/darkness cycle), 22°C, with food

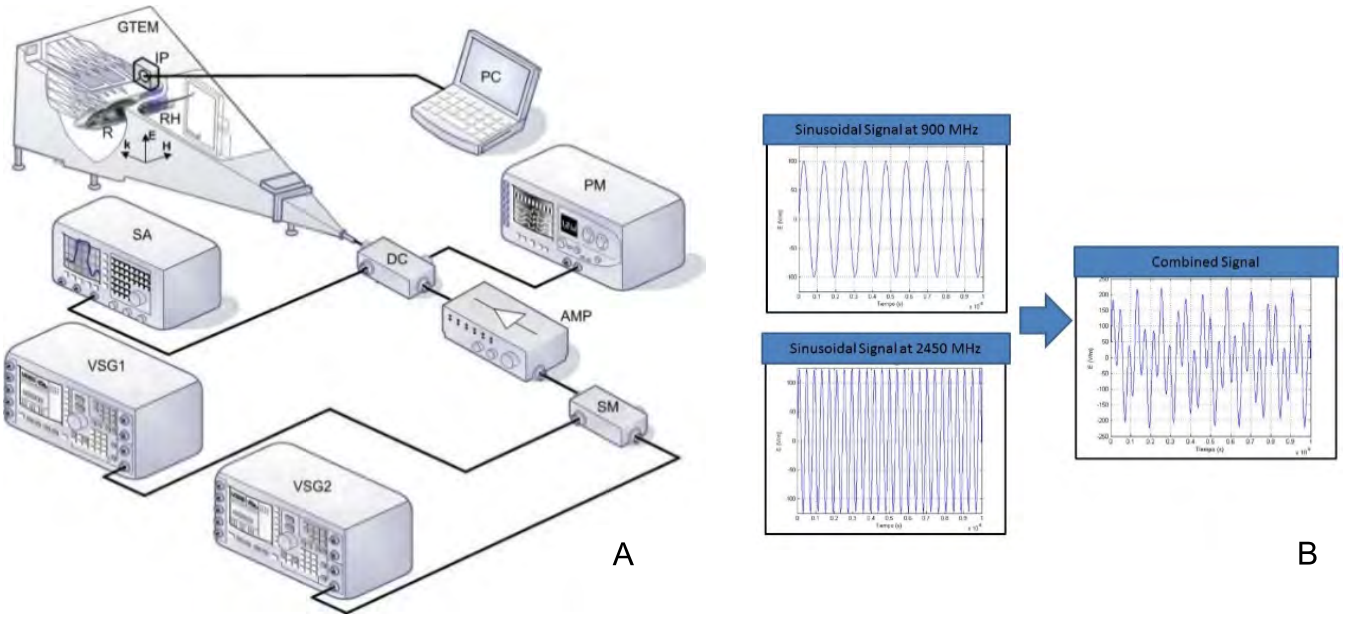

FIGURE 4. A) Diagram of Experimental System III. GTEM, Schaffner 250 GTEM chamber; VSG1, Agilent E8267D Vector Signal Generator (250 KHz–20 GHz) operating at 2.45 GHz; VSG2, Agilent E4438C Vector Signal Generator (250 KHz–4 GHz) operating at 900 MHz; AMP, Research Amplifier 15S1G3 (0.8–3 GHz); DC, NARDA 3282B-30 Directional Coupler (800–4000 MHz); SA, Agilent E4407B Spectrum Analyzer (9 KHz–26.5 GHz); PM, Agilent E4418B Power Meter; SM, Signal Mixer (Agilent 11636a power divider used as a power combiner); RH, rat holder; IP, EMF Cube Isotropic Probe; R, rat. B) Representation of each of the pure sinusoidal signals used (900 MHz and 2.45 GHz) and the sum of both signals (900 + 2.45 GHz).

TABLE 1. Experimental design and management of the animals: A summary of the experimental methodology and the animal model used for each case are shown.

EXPERIMENTAL MODEL	ANIMALS	PHARMACOLOGICAL MANIPULATION	PROTOCOL OF EXPOSURE		CLINICAL BEHAVIOUR/EEG	TIME POST EXPOSURE (h)	PUBLICATIONS
			TYPE	TIME (h)			
Seizure prone rat model	Male Sprague-Dawley rats	Inject picrotoxin (2mg/kg)	Unique	2.0	Electroencephalogram Videotaped	1.5 24.0 72.0	**14,15,16,17,20,21**
Diathermy rat model	Female Sprague-Dawley rats	-	Unique Repeated (10 times)	0.5	-	1.5 24.0	**24,25,26,27,28**
Rat model in two combined frequencies	Male Sprague-Dawley rats	-	Unique	1.0 2.0	-	1.5 24.0	**29,30**

and water. In all the cases the animals were individually immobilized in a methacrylate holder during the radiation process. Likewise, also control animals were immobilized in same conditions as radiated animals. Some of these animals were pharmacologically manipulated in a previous stage to the radiation process. Also, it is important to note that EEG measurements and video camera recording were made during the radiation stage to evaluate the appearance of convulsions or myoclonic head and body jerks (see Table 1). Otherwise, the rectal temperature was registered in most part of the studies due to the fact that it represents a good indicator of the absorption of the electromagnetic radiation (see Table 2).

All the experiments were carried out by following the guidelines of the European animal protection regulations (Directive 86/609l), the current Spanish directive RD1201/2005, the Declaration of Helsinki and the guide for the care and use of laboratory animals, as it was adopted and promulgated by the US National Institute of Health (NIH Publication No. 85-23, revised 1996). All the experimental protocols were approved by the Bioethics Committee on the Use and Care of Animals of the University of Santiago de Compostela.

IV. SAR CALCULATION TECHNIQUES

A. STANDING WAVE CAVITY PROBLEM

We calculated the SAR (Specific Absorption Rate) values in the standing wave cavity problems through simulation of the $|E|$ field distribution within the radiation region, with the animal model and the antennas optimally placed as indicated. In the simulation, the antennas were considered as $\lambda/4$, and we used a single 198.3 g numerical model (SPEAG SEMCAD numerical phantom) for the rat. The

TABLE 2. Information about the subthermal radiation in the animals: A summary of the dosimetry and temperature measurements related with each experiment are shown.

EXPERIMENTAL MODEL	FREQUENCY (MHz)	MEAN SAR (W/Kg)	MEASUREMENT OF RECTAL TEMPERATURES	PUBLICATIONS
Seizure prone rat model	900 GSM	**Head** 0.27- 1.36 **Body** 0.15- 0.76	-	**15,16,17,20,21**
Diathermy rat model	2450	**Head** 0.2-0.9 **Thyroid** 0.04-0.4 **Thymus** 0.04-0.48 **Body** 0.04-0.79	Significant differences before and after radiation only for 12W.	**24,25,26,27,28**
Rat model in two combined frequencies	900; 2450; 2450 + 900	**Cerebrum** 0.058-0.07; 0.27-0.32; 0.02-0.15 **Cerebellum** 0.02-0.04; 0.15-0.17; 0.06-0.08 **Body** 0.054-0.087; 0.07-0.09; 0.047-0.07	Significant differences before and after radiation only with 2W.	**29,30**

model rat consisted of 60 different tissues based on scanned MRI sections (1.15 mm width). The simulation SAR value was then normalized to the experimental absorbed power value for each animal. By adjusting the simulated values to the actual weight of the rats and the actual absorbed power, we obtained an estimated specific absorption ratio, SAR_E, for the experimental animals, which can be expressed as

$$SAR_E = SAR_S \times \frac{P_{A,E}}{P_{A,S}} \times \frac{W_S}{W_E} \quad (1)$$

where:

SAR_S = Simulated SAR
$P_{A,E}$ = Power absorbed by the rat (Difference in the power dissipated in the cavity with and without the rat inside the RH)
$P_{A,S}$ = Power absorbed by numerical rat
W_E = Weight of rat
W_S = Weight of simulated rat

The values of sub-thermal SAR in the radiated animals which were obtained in the experiments carried out in this cavity are in Table 2.

B. TRAVELLING WAVE CAVITY PROBLEM: WEIGHT RATIO

In each case, the electric field value from the simulation was experimentally verified with an isotropic probe placed in the center of the exposure area.

We estimated SAR_E by applying a correction factor, based on the ratio of model rat weight to experimental rat weight, to the numerical simulation values, expressed as

$$SAR_E = SAR_S \times \frac{W_S}{W_E} \quad (2)$$

where SAR_S is the SAR obtained from the simulation, W_S is the weight of the model rat, and W_E is the weight of the experimental rat.

C. TRAVELLING WAVE CAVITY PROBLEM: SCALING THE MODEL

SAR_E was estimated by scaling the SEMCAD numerical model rat and adjusting it for weight differences among the experimental rats in the radiated animal groups. To achieve uniform scaling, we multiplied all the original dimensions of the voxels that are included in the numerical phantom of the rat by the proportionality constant that was required for effectively scaling the rat model to a model that [10].

The values related with the sub-thermal SAR also for this case can be found in Table 2.

V. EXPERIMENTAL VALIDATION OF RAT BIOLOGICAL MODELS

A. MODEL FOR SEIZURE PRONE RATS IN STANDING-WAVE CAVITY

Experimental studies in this group began with the hypothesis that modulated GSM radiation at sub-thermal SAR levels could increase electrical instability in brain tissue of rats that had been made seizure-prone through injection of a sub-convulsive (not inducing spontaneous seizures) dose of the γ-aminobutyric acid (GABA) antagonist picrotoxin [7].

In the first study, we assessed the effects of the radiation by observing (with electroencephalography in some cases), whether the rats suffered seizures or not. We also did post mortem immunochemical analyses of relevant brain areas based on the presence of c-Fos, a sensitive marker of neuronal activation [11] that appears in brain areas affected by seizures [12]. The rats were exposed for 2h to GSM pulse modulation [13] radiation at 900 MHz, with SAR values of 0.27 W/kg and at an intensity comparable to that of mobile phone emissions [14].

EEGs (Electroencephalograms) indicated that the irradiated picrotoxin-treated rats suffered seizures featuring generalized, continuous spike-and-wave trains. Non-treated rats presented no abnormal activity or indications of seizure, and spikes did not appear in the EEG recordings from these groups.

C-fos levels significantly higher in irradiated picrotoxin-treated animals than in non-irradiated picrotoxin-treated ones

in the neocortex (frontal cortex, parietal cortex), the paleocortex (piriform cortex, entorhinal cortex) the hippocampus (dentate gyrus, hippocampal CA1; hippocampal CA3) and the thalamus (Centrolateral nuclei, Centromedial nuclei). In these regions, however, no significant differences in c-fos counts appeared between irradiated rats and non-irradiated rats that had not received picrotoxin.

The results of this study, in which clinical observation was combined with EEG recordings and immunohistochemical assays, give strong indication that GSM radiation can significantly modify activity in cerebral tissues with GABAergic circuits that are already in an altered condition [14].

The design of the metal chamber and the radiation distribution within it made it possible to observe the effects of repeated exposure on the body of the animal, which was positioned to receive maximum radiation level to the head [15], [16].

The rats presented indicators (clinical, EEG, neuronal activity) of alterations in brain activity that could not be attributed to the effect of heating, as the SAR (Specific Absorption Rate) was too low to induce generalized heating of tissues. This suggested that modulated GSM radiation could impact brain activity.

Those findings led to a second experiment, in an attempt to explain whether pulse-modulated GSM affected brain activity differently than unmodulated radiation at identical wavelengths. In this study, EEG signals and c-Fos expression in the brains of picrotoxin-pretreated rats exposed to modulated GSM presented clinical differences to those of picrotoxin-treated rats exposed to the same dose of unmodulated radiation [17]. The first group displayed myoclonic head and body jerks that continued for long time periods, along with sporadic general convulsions. Picrotoxin-treated rats exposed to unmodulated radiation presented occasional myoclonic head jerks and forepaw spasms, but only one animal suffered generalized seizures. EEG recordings showed short polyspikes or continuous spike-and-wave discharges during seizure activity. Non-picrotoxin-treated GSM-irradiated or unmodulated-irradiated rats presented no indications of myoclonic jerks or abnormalities in the EEG recordings. These findings of seizures with GSM and the near absence of clinical or EEG symptoms without GSM suggest that there is some synergic relations or facilitations between the effects of the convulsant drug picrotoxin and GSM radiation. Also, these findings can suggest that they are induced through a common mechanism. Similar findings have been reported for other drugs [18] (see Table 3).

The effects of GSM radiation on c-Fos expression in picrotoxin-treated rats were most pronounced in the limbic structures, areas of the olfactory cortex, the subcortex, the dentate gyrus, and the central lateral nucleus of the thalamic intralaminar nucleus group. Picrotoxin-treated groups showed significant differences in c-Fos expression between the GSM irradiated group and the unmodulated irradiated group. However, no significant differences appeared in c-Fos expression between picrotoxin-treated and non-picrotoxin-treated rats exposed to unmodulated radiation. Table 4 in [17] shows these above-mentioned results. Our findings suggest that pulse modulation acts as a trigger for seizures and increased c-Fos levels, pointing to the existence of a mechanism that is not affected by changes in temperature [19].

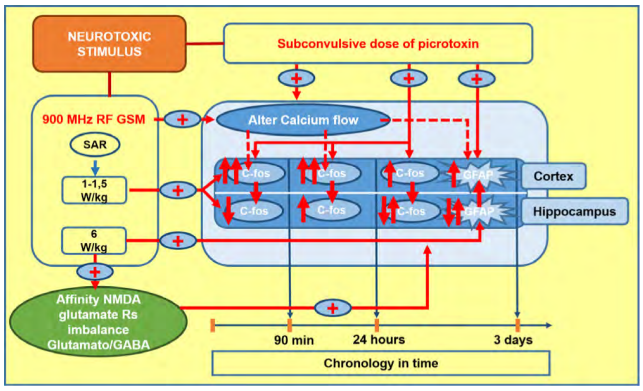

FIGURE 5. Illustration of the assumed link between GSM radiation and pathological findings for the cortex and hippocampus. Summarized here are the effects on the c-Fos neuronal marker and the GFAP glia marker, stemming from radiation (SAR 1.0 to 1.5 W/kg) and picrotoxin (2 mg/kg), in relation to time after exposure (90 min, 24 hours, 3 days). Red arrows indicate ongoing activation of different mechanisms. Dashed red arrows indicate hypotheses of possible triggers.

The simple picrotoxin model that we have developed in our laboratory made it possible to identify morphological signs of neurotoxicity in rat brain tissue. This may directly affect our understanding of risk related to exposure to RF radiation in patients with epilepsy [14], [16], [17].

In the next experiment, we used positive immunochemical testing for neuronal (c-Fos) and GFAP (Glial Fibrillary Acid Protein) cells to look for indications of neural stress in cerebral activity after exposure to modulated GSM radiation at 900 MHz in a picrotoxin-treated. We recorded the chronological response cascade at 90 minutes, 24 hours and 72 hours after acute exposure [20].

Ninety minutes after radiation, we observed elevated c-Fos expression in the neocortex and paleocortex, accompanied by low activation of the hippocampus in picrotoxin-treated rats. Except in the limbic cortex, neuronal activation had increased notably in most brain areas 24 hours after picrotoxin and radiation. Three days after exposure, the effects of radiation in picrotoxin-treated animals were still evident in the neocortex, dentate Gyrus and CA3 but activity had decreased significantly in the piriform and entorhinal cortex. Meanwhile, glial reactivity in brain regions of irradiated, picrotoxin-treated rats had increased with every seizure. All these above-mentioned results are included in Table 8 of [20]. In the seizure model used for this study, the GABA-A channels become blocked and the glutamatergic system overrides the GABAergic inhibitor system, which entails an increase in neuronal activation. Apparently, this activation of the NMDA receptors in the astrocytes explains glial activation in the presence of picrotoxin (see Fig. 5 and Table 3).

TABLE 3. Summary of the obtained results from publications for the experimental model used on each case.

EXPERIMENTAL MODEL	CLINICAL BEHAVIOUR AND EEG RESULTS	ELISA,HISTOPATHOLOGY RESULTS	CONCLUSIONS	PUBLICATIONS
Seizure prone rat model	75% of rats (picrotoxin treated/GSM-irradiated) showed seizures and generalized continuous spike-and-wave trains during seizures	**Neuronal activity:** 55% more mean positivity with picrotoxin and GSM radiation than with picrotoxin and unmodulated radiation for c-FOS cells in brain (cortex and midbrain). **Glial proliferation:** 15% more mean GFAP-positivity cell count in cerebral cortex with picrotoxin and GSM radiation.	900 MHz-GSM radiation triggered a marked increase in neuronal excitability in seizure-prone rats. Glial proliferation. Evidence of neurotoxicity in the brain: cortex and midbrain depending on SAR value.	**15,16,17,20,21**
Diathermy rat model	-	**Brain:** Changes in the levels (Increase or decrease) and distribution of HSP-90. No apoptotic cellular nuclei and some DARK neurons. Repeated exposure to radiation at 3 W increased cellular activation in the PVN by over 100% compared to animals exposed to acute irradiation and repeated-irradiation exposure non-radiated control animals. **Thyroid:** Decrease HSP-90/70 without apoptotic signs. Variation in expression and distribution of HSP-90 in follicular, parafollicular cells, follicular and capsular membranes. Increase in follicle diameter (25-30%), decrease in septa thickness (21-26%). **Thymus:** Decrease in HSP-90 and minimal marked in capsule/membrane with maximum power. No significant differences in HSP-70. Increase in red blood cells (2-5 times), blood vessels (2-5 times), epithelial reticular cells (4 times) and glucocorticoid receptors (2-3 times) with maximum power. PLS regression showed that the results depended mainly on the power of the radiation.	2450 MHz radiation induces changes in the distribution cytoplasmic chaperones of nerve cells, thyroid cells and thymus cells without signs of lesion or apoptosis. In thyroid gland provokes hypertrophy related to the SAR and/or number of exposures. In thymus there is a relationship between power radiation and increase in endothelial permeability and vascularization of the thymus and glucocorticoid receptors. The radiation constitutes a stimulus for immune response.	**24,25,26,27,28**
Rat model in two combined frequencies	-	No lesions were shown. Tissue destruction and apoptosis in the cerebral cortex, cerebellum, pituitary gland, tongue, trapezoid muscle, thymus interscapular fat and a testicle with power of 2W. Significant differences were evident in HSP-90/70 but not in Caspase-3 levels between the hemispheres of the cerebral cortex at high SAR levels. In the cerebellar hemispheres, groups exposed to a single radiofrequency (RF) and high SAR showed significant differences in HSP 90/70 and Caspase-3 levels compared to control animal	The absence of acute tissue effects to the two-frequency signal (900 MHz and 2450 MHz) on the cells of these nine tissues in comparison with the effects of the single-frequency signals, gamma radiation, or non-exposure. The biological effect of cellular stress in the cerebral cortex and/or cerebellum is related to the nature of the signal than any additive action of the two combined frequencies.	**28,29**

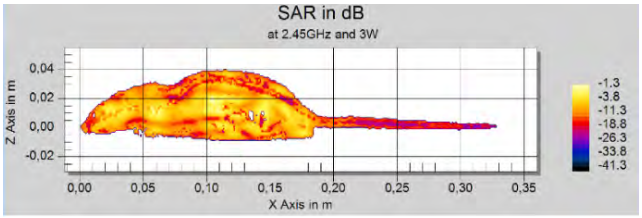

FIGURE 6. Distribution of local SARs in the phantom rat 'exposed' to 2.45 GHz at 3 W, in the plane X = 0:33 m.

Despite the ponderous anatomical differences between rats and humans with regard to brain size, morphology, and therefore dosimetry, we found that the combination of stress from non-thermal SAR due to radiation and the noxious action of picrotoxin activated c-Fos protein and glia markers in brain tissue. Since nervous pathways in persons with epilepsy tend towards electrical instability, our findings suggest that this group may be especially sensitive to electromagnetic radiation [21].

B. EXPERIMENTAL CELLULAR STRESS AND DIATHERMIC MODEL IN TRAVELLING WAVE CAVITY AT SINGLE FREQUENCY

Burgeoning use of 2.45GHz electromagnetic fields in industry and medicine, in Bluetooth wireless technologies [22] and in rehabilitation therapies for diverse categories of pain and pathology [23] led us on a quest to find new laboratory models for studying cellular stress in relation to non-ionizing radiation at subthermal SAR levels.

We began studying quantitative and qualitative expression of HSP-90 in different anatomical regions of the rat brain following acute exposure of Sprague-Dawley rats to 2.45 GHz radiation at different SAR in a GTEM chamber (see Table 3). We also examined morphological lesions in histopathological sections from these animals to look for dark neurons or DAPI-stained nuclei. The study was designed to look for changes in expression of HSP-90, a biological marker in the brain including regional differences and alterations in the cytoprotective effect of this molecular chaperone in reaction to non-ionizing radiation [24]. Following exposure to radiation, cellular distribution of HSP-90 increased with higher SAR in the hypothalamic nuclei, limbic cortex and somatosensorial cortex. Twenty-four hours after irradiation, HSP-90 levels remained high in all hypothalamic nuclei for all SAR. In the parietal cortex, HSP-90 levels remained high compared to non-radiated animals 24 hours after exposure. However, in the limbic system, HSP-90 levels were significantly lower (nearly half) than in non-radiated animals 24 hours after exposure at the highest power. Non-apoptotic cellular nuclei and dark neurons were present 90 minutes and 24 hours after maximum SAR exposure.

The next experiment was a comparative analysis of how cellular activation resulting from non-pulsed electromagnetic fields applied at 2.45 GHz and 3 or 12 W affected the paraventricular nucleus (PVN) which in rats is located in the anterior hypothalamus. The animals underwent single 30 min

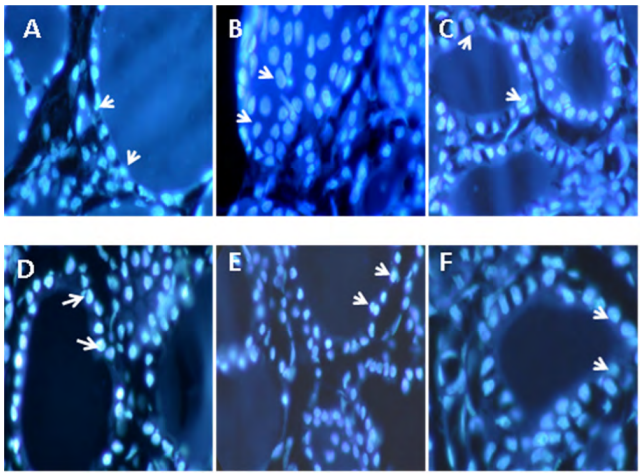

FIGURE 7. Rat thyroid tissue stained with fluorescent DAPI. The photographs show no nuclear fragmentation or chromatin condensation in the epithelial cells of the thyroid follicles in any of the experimental groups. Photos (A) (B) (C): Animals slaughtered 24 h after exposure to 0 W (control), 1.5 W or 12 W, respectively; (D) (E) (F): Animals slaughtered 90 min after exposure to 0 W (control), 1.5 W or 12 W. Arrows indicate follicular cells with no signs of apoptosis. 100× magnification, calibration bar 20 μm.

exposure or repeated exposure (30 min exposure at 3 W for 10 sessions in a two-week period) in a GTEM chamber [25]. High SAR provoked an increase of the c-Fos marker 90 min or 24 h after radiation, but with low SAR, c-Fos counts were higher than in control rats after 24 h. Repeated irradiation at 3 W (see SAR, Fig. 6) increased cellular activation in the PVN by over 100% compared to animals exposed to acute irradiation and repeated-exposure non-radiated control animals (see Table 3).

Several recent studies have described the relationship between RF exposure and thyroid gland disorders. We developed an experiment to determine HSP-90 and HSP-70 levels for analyzing cellular stress from radiation. We exposed female rat thyroid tissue to 2.45 GHz RF in an experimental GTEM system [26] to study the effects on anti-apoptotic activity and integrity.

HSP-90 and HSP-70 had significantly decreased ninety minutes after applying radiation at 0.04 W/kg or 0.10W/kg SAR (see Fig. 2 in [26]). Twenty-four hours after radiation, HSP-90 had partially recovered and HSP-70 had completely recovered. Signs of lesions were scarce in the gland and there were no indications of apoptosis in any of the radiated animals. Our findings suggest that acute sub-thermal radiation at 2.45 GHz could alter cellular stress levels in rat thyroid gland without affecting anti-apoptotic capacity at first (see Fig. 7).

In human environments, exposure to direct and indirect non-ionizing radiation is common. Despite indications that radiation triggers stress in thyroid cells, little research has been done on morphological changes that signal precocious re-adjustments in the mammalian thyroid gland after close-range exposure to non-ionizing radiation at 2.45 GHz. Our next study involved a diathermic model and experimental set-up that focused maximum direct radiation on the

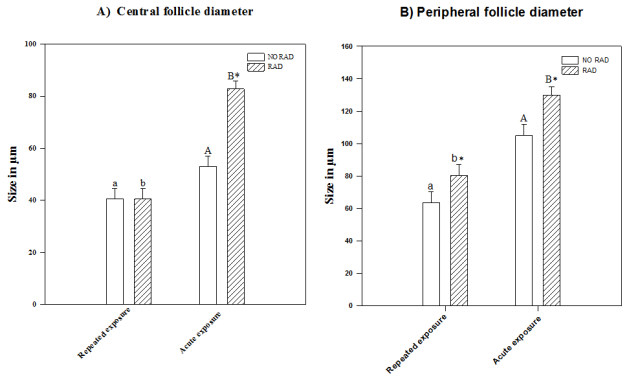

FIGURE 8. No significant differences were detected in central follicle diameter size, but the diameter of the peripheral follicle increased significantly in animals exposed repeatedly compared to non-radiated animals. An asterisk * indicates statistically significant differences between radiated/non-radiated; a, b indicate statistically significant differences between rats that underwent repeated exposure versus single exposure ($p<0.05$, two-way ANOVA, followed by Tukey's test).

left shoulder of the animal, which was immobilized inside a GTEM chamber. According to our hypothesis, exposure to localized 2.45 GHz diathermic radiation would trigger detectable changes in thyroid gland morphology and alterations in the expression of heat stress proteins in rat thyroid cells. We tested the hypothesis through immunohistochemical assay of HSP-90 expression in rat thyroid tissue after single or repeated (10 times in two weeks) exposure to 2.45 GHz RF and looked for morphological changes. The radiation levels, exposure time, and doses were on a human scale [27]. After ninety minutes of radiation with the highest SAR, the central and peripheral follicles had become enlarged and the peripheral septa had become thinner. Twenty-four hours after exposure, only the central follicles radiated at 12W were observed to be smaller, while peripheral follicles exposed repeatedly at 3W had increased in size (see Fig. 8). In this diathermy experiment, rat thyroid exposed to 2.45 GHz radiation showed visible morphological effects including: (a) hypertrophy of the gland linked to SAR and/or number of exposures; (b) changes in HSP-90 distribution in membranes and parafollicular cells. It is inconclusive whether these effects were the direct or exclusive result of radiation, so they can be listed among indirect effects on the hypothalamus (see Table 3).

Electromagnetic fields can induce or mediate stress response by triggering the production of HSPs, which regulate immune response and thymus function. To better understand this process, we studied cellular stress in rat thymus after exposure to RF at 2.45 GHz, based on an experimental diathermic model in a GTEM chamber. We analyzed HSP-70 and HSP-90 as indicators of cellular stress and glucocorticoid receptor expression, applying a hematoxylin-eosin (H&E) stain that made histological and immunohistochemical changes easier to detect [28]. Among the morphological variations observed in the thymus tissue were augmented blood vessel distribution and the presence of red blood cells as well as hemorrhagic reticuloepithelial cells. HSP-90 decreased in the thymus of rats exposed to the highest power level (12 W), but all groups except one recovered after 24 h. There were no significant alterations of HSP-70 in any group. Finally, glucocorticoid receptor immunomarkers were more prevalent in the thymic cortex of exposed rats (see Table 3).

C. MALE RAT MODEL IN TRAVELLING WAVE CAVITY WITH TWO COMBINED FREQUENCIES

We began studying exposure to simultaneous multiple RF signals in order to experimentally observe tissue condition and apoptosis status in exposed rats and to look for correlations between tissue damage and SAR-based estimates. Sections of different tissues (cerebral cortex, cerebellum, thymus, pituitary gland, tongue, trapezoid muscle, testicle, interscapular fat) were taken from rats sacrificed 24 h after exposure, as well as from negative controls and positive controls exposed to gamma radiation. The tissues were stained with haematoxylin-eosin to facilitate examination of general cell morphology and with DAPI to identify apoptosis [29]. Only the positive controls presented lesions or indications of tissue destruction or apoptosis. The results for rats exposed to either frequency, or to both at the same time, were quite similar to the results for the negative controls. The low specific absorption rates applied in the experiment (< 0.3 W/kg except in the pituitary glands), along with single rather than repeated exposure in the design, may have been responsible for lack of significant effects. The study did not clarify: 1) additivity of absorbed energy and/ or biological effects in tissue or 2) whether combined and single frequencies have the same interaction mechanism in live tissue. These unanswered questions led to another experiment, in which Sprague-Dawley rats were irradiated in an experimental multifrequency system and the combined SAR was determined by FDTD. We then looked at cellular stress based on expression of HSP 90 and 70 and examined both hemispheres of the cerebrum and cerebellum for effects of pre-apoptotic caspase-3 activity [30].

Twenty-four hours after exposure to combined or single radiation, we observed significant differences in HSP-90 and HSP-70 expression. However, there were no significant differences in caspase 3 levels between the hemispheres of the cerebral cortex at high SAR levels. In the cerebellar hemispheres, groups exposed to a single RF and high SAR displayed significant differences in the expression of HSP-90, HSP-70 and caspase-3 with respect to control animals. This indicates that absorbed energy and/or biological effects of combined signals were not additive, by which we deduce that another mechanism is involved when multiple frequencies interact with nervous tissue (see Table 3).

VI. DISCUSSION AND DIRECTIONS FOR FUTURE RESEARCH.

This publication analyzes the impact on human health of experimental studies of radiofrequency exposure in animals; however, it should be taken into account that they

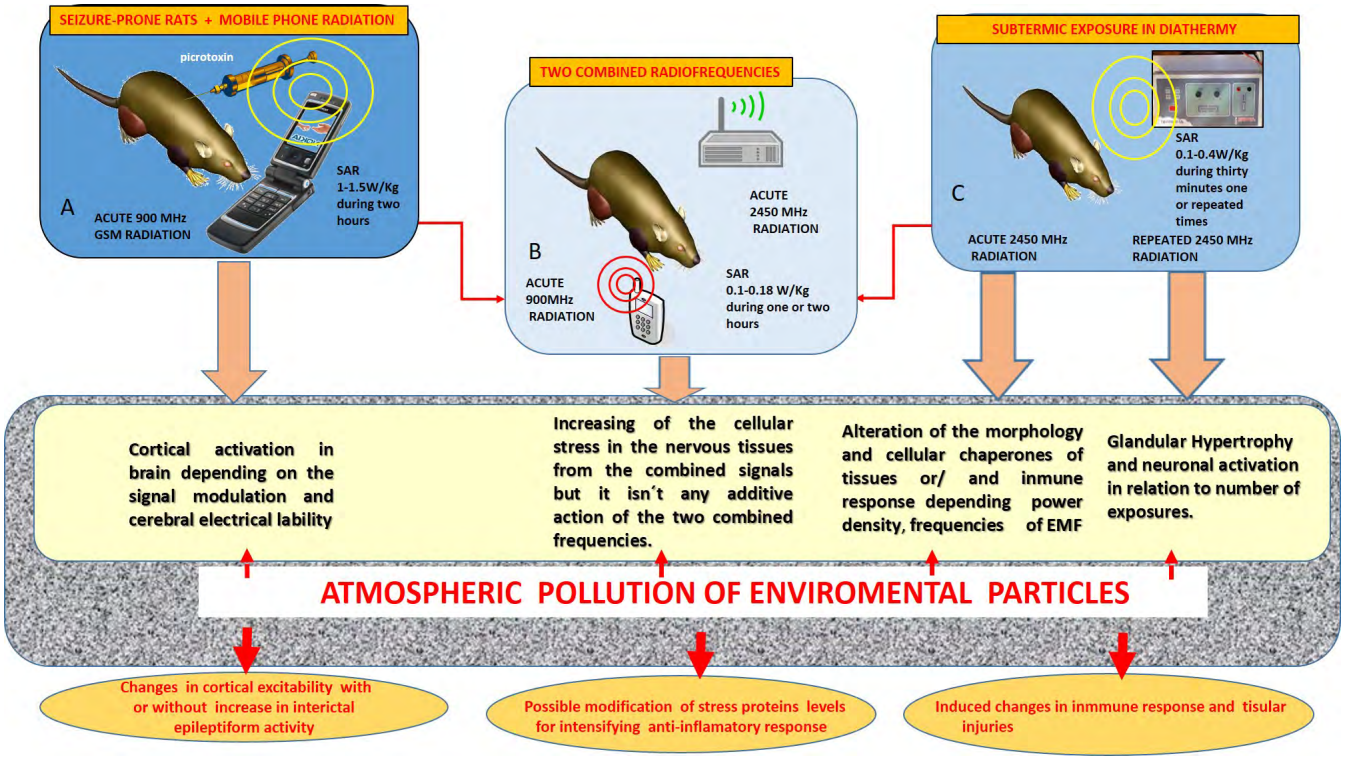

FIGURE 9. Sketch of our hypothesis about the role which the particulate matter atmospheric pollution play in the experimental models for animals exposed to non-ionizing radiation is here depicted. The pictures A, B, C are the sketches of the three EM models in which the studied animals are introduced. Through orange wide arrows the more relevant facts of each study are stated. The wide red arrows suggest the possible biological effects induced by means of the combination of the EM radiation and the particulate matter pollution on each case.

were carried out in short periods of time in both acute and subacute manner. The lack of more long-term studies prevents having incomplete information on the impact of non-ionizing radiation on the health of the population. However, it does not de-authorize the study as the validation and analysis of short-term biological effects since they could provide relevant information about the risks and initial mechanisms of interaction of electromagnetic field with the population.

Several studies in humans validate our findings based on experimental radiation systems with animals: modifications of the EEG activity in epileptic patients [31]–[34], hormonal alterations or increasing in thyroid cancer [35], [36], and neurological symptomatology provoked by means of the interaction of multiple radiofrequencies [37].

GSM radiation (in a standing wave cavity) at 900 MHz can induce seizures in rats made susceptible to seizures through the administration of picrotoxin in subconvulsive doses. Behavioral indicators, EEG results and c-Fos expression in neurons confirmed this in comparison to rats exposed to unmodulated radiation. GFAP and c-Fos, which are positive neurotoxic markers, induced potentially reversible alterations in brains with a physiological tendency towards electrical instability. Our findings underscore the relevance of further rigorous research to understand the effects of mobile telephone RF on persons suffering from epilepsy. Forty-five minutes exposure to GSM-EMFs of a mobile phone modulates the inter-hemispheric coupling of resting EEG rhythms in epilepsy patients [32]. However, a significant increase in EEG activity within the alpha, beta, and gamma bands is also described when epileptic patients were exposed to controlled electromagnetic radiation in a controlled manner [31].

Environmental risk factors, such as air pollution, could potentially impact large sections of the population and there is become public health concerns. The exposure to environmental factors has been shown to increase the risk the hospitalization for epilepsy [38]. The crucial role of several possible mechanisms which modify cortical excitability which would act simultaneously in this pathology it is now undetermined (see Fig. 9).

However, as a consequence of the urbanization progress, the particulate matter pollution in the atmosphere represents an important risk for the development of diseases and/or cancer [39]–[41]. In other hand, the exposure to electromagnetic fields induce either stimulatory, inhibitory, or no effect on the immune system in relationship to how specific EMF frequencies, specific EMF power densities, and specific EMF durations interact with specific field parameters [42].

From the citizen health care point of view, to breathe polluted air modifies the immune response and increases the systemic effects and injuries in the tissues [43], [44]. The design of experimental models in which various toxic agents are combined and interact between them could help to understand the pathogeny of several diseases (see Fig. 9).

Combined radiation at 900 and 2.45 GHz RF subthermal SAR in a GTEM chamber apparently had no negative effects on tissues; the results were comparable to those of non-radiated animals. The combined signals triggered energy absorption in nervous tissue at 2W or 4 W power, but the absorbed energy did not correspond to the sum of the two SARs. Cellular stress in the cerebral cortex, the cerebellum or both seems to be more associated with the type of signal than with additive effects of combined frequencies. This points to the possibility of another mechanism at work when multiple signals act on tissue. Consequently, there is no linear cause-effect relationship, the sub-thermal effects from a combined two-frequency signal must be described as a non-linear study biosystem.

The electromagnetic pollution is essentially concentrated in urban areas: there are some evidences about it can augment the effects of certain other pollutants, e.g. by enhancing metal-induced cellular stress and oxidative stress [45]. Endoplasmic reticulum stress and the unfolden protein response can trigger cell death in illnesses which are associated with early mortality and PM exposure; therefore, endoplasmic reticulum stress is a plausible mechanism of PM-mediated inflammation and adverse health effects [46].

Simultaneous exposure to particulate and electromagnetic air pollution can have synergistic effects on the nervous system (see Fig. 9).

VII. CONCLUSIONS

The experimental models of controlled exposure of animals to radiofrequency allow us to know in the short term the mechanisms and risks that can affect human health. The modulation of EEG rhythms in epileptics, the modification of the immune response and the increase in cellular stress are biological effects that could be caused in humans by radio frequency interaction. In an urban environmental that combines the electromagnetic and chemical pollution of environmental particles cortical excitability, inflammatory response and cell injury can be modified.

REFERENCES

[1] A. B. Miller, L. L. Morgan, I. Udasin, and D. L. Davis, "Cancer epidemiology update, following the 2011 IARC evaluation of radiofrequency electromagnetic fields (Monograph 102)," *Environ. Res.*, vol. 167, pp. 673–683, Nov. 2018.

[2] S. J. Regel and P. Achermann, "Cognitive performance measures in bioelectromagnetic research-critical evaluation and recommendations," *Environ. Health*, vol. 10, no. 1, pp. 1–10, 2011.

[3] Y. B. Jin, H. J. Lee, J. Seon Lee, J. K. Pack, N. Kim, and Y. S. Lee, "One-year, simultaneous combined exposure of CDMA and WCDMA radiofrequency electromagnetic fields to rats," *Int. J. Radiat. Biol.*, vol. 87, pp. 416–423, Apr. 2011.

[4] Ö. Sangün, B. Dündar, S. Çömlekçi, and A. Büyükgebiz, "The effects of electromagnetic field on the endocrine system in children and adolescents," *Pediatric Endocrinol. Rev.*, vol. 13, no. 2, pp. 531–545, 2015.

[5] I. Belyaev, A. Dean, H. Eger, G. Hubmann, R. Jandrisovits, M. Kern, M. Kundi, H. Moshammer, P. Lercher, K. Müller, and G. Oberfeld, "EUROPAEM EMF guideline 2016 for the prevention, diagnosis and treatment of EMF-related health problems and illnesses," *Rev. Environ. Health*, vol. 31, no. 3, pp. 363–397, 2016.

[6] Y.-H. Hao, L. Zhao, and R. Y. Peng, "Effects of microwave radiation on brain energy metabolism and related mechanisms," *Mil. Med. Res.*, vol. 2, no. 4, pp. 1–8, 2015.

[7] D. J. Nutt, P. J. Cowen, C. C. Batts, D. G. Grahame-Smith, and A. R. Green, "Repeated administration of subconvulsant doses of GABA antagonist drugs. I. Effect on seizure threshold (kindling)," *Psychopharmacology*, vol. 76, no. 1, pp. 84–87, 1982.

[8] S. C. Gupta, A. Sharma, M. Mishra, R. K. Mishra, and D. K. Chowdhuri, "Heat shock proteins in toxicology: How close and how far?" *Life Sci.*, vol. 86, nos. 11–12, pp. 377–384, 2010.

[9] H. J. Lee, Y.-B. Jin, T.-H. Kim, J.-K. Pack, N. Kim, H.-D. Choi, and Y.-S. Lee, "The effects of simultaneous combined exposure to CDMA and WCDMA electromagnetic fields on rat testicular function," *Bioelectromagnetics*, vol. 33, no. 4, pp. 356–364, 2012.

[10] F. Schönborn, K. Poković, and N. Kuster, "Dosimetric analysis of the carousel setup for the exposure of rats at 1.62 GHz," *Bioelectromagnetics*, vol. 25, no. 1, pp. 16–26, 2004.

[11] J. I. Morgan and T. Curran, "Stimulus-transcription coupling in the nervous system: Involvement of the inducible proto-oncogenes fos and jun," *Annu. Rev. Neurosci.*, vol. 14, no. 1, pp. 421–451, 1991.

[12] J. O. Willoughby, L. Mackenzie, A. Medvedev, and J. Hiscock, "Distribution of FoS-positive neurons in cortical and subcortical structures after picrotoxin-induced convulsions varies with seizure type," *Brain Res.*, vol. 683, no. 1, pp. 73–87, 1995.

[13] I. Poole, *Cellular Communications Explained: From Basics to 3G*, 1st ed. Amsterdam, The Netherlands: Elsevier, 2006.

[14] E. López-Martín, J. L. Relova-Quinteiro, R. Gallego-Gómez, M. Peleteiro-Fernández, F. J. Jorge-Barreiro, and F. J. Ares-Pena, "GSM radiation triggers seizures and increases cerebral c-Fos positivity in rats pretreated with subconvulsive doses of picrotoxin," *Neurosci. Lett.*, vol. 398, nos. 1–2, pp. 139–144, 2006.

[15] E. López-Martín, J. L. Relova-Quinteiro, J. C. Bregains, and F. J. Ares-Pena, "Acute exposure to a standing wave GSM-like mobile phone signal in rats treated with subconvulsive doses of picrotoxin: Effects on cerebral activity," in *Mobile Telephones: Networks, Applications, and Performance*. New York, NY, USA: Nova, 2008, ch. 9, pp. 241–251.

[16] E. López-Martín, J. C. Bregains, F. J. Jorge-Barreiro, J. L. Sebastián-Franco, E. Moreno-Piquero, and F. Ares-Pena, "An experimental set-up for measurement of the power absorbed from 900 MHz GSM standing waves by small animals, illustrated by application to picrotoxin-treated rats," *Prog. Electromagn. Res.*, vol. 87, pp. 149–165, 2008.

[17] E. López-Martín, J. Bregains, J. L. Relova-Quintero, F. J. Jorge-Barreiro, and F. J. Ares-Pena, "The action of pulse-modulated GSM radiation increases regional changes in brain activity and c-Fos expression in cortical and subcortical areas in a rat model of picrotoxin-induced seizure proneness," *J. Neurosci. Res.*, vol. 87, no. 6, pp. 1484–1499, 2009.

[18] S. M. Michaelson, C. E. Elson, and C. L. Anderson, "Interaction of non-modulated and pulse modulated radiofrequency fields with living matter: Experimental results," in *Biological and Medical Aspects of Electromagnetic Fields* (Handbook of Biological Effects of Electromagnetic Fields), 3rd ed. New York, NY, USA: CRC Press, 2006, ch. 3, pp. 53–147.

[19] C. Curcio, M. Ferrara, F. Moroni, G. D'inzo, M. Bertini, and L. De Genaro, "Is the brain influenced by a phone call?: An EEG study of resting wakefulness," *Neurosci. Res.*, vol. 53, no. 3, pp. 265–270, 2005.

[20] M. Carballo-Quintás, I. Martínez-Silva, C. Cadarso-Suárez, M. Alvarez-Folgueiras, F. J. Ares-Pena, and E. López-Martín, "A study of neurotoxic biomarkers, c-Fos and GFAP after acute exposure to GSM radiation at 900 MHz in the picrotoxin model of rat brains," *Neurotoxicology*, vol. 32, no. 4, pp. 478–494, 2011.

[21] E. López-Martín and F. J. Ares-Pena, "An evaluation of neurotoxicity markers in rat brains, using a pre-convulsive model and exposure to 900 MHZ modulated GSM radio frequency," in *Electromagnetic Fields: Principles, Engineering Applications and Biophysical Effects*, New York, NY, USA: Nova, 2013, ch. 10, pp. 331–347.

[22] M. Otto, and K. E. von Mühlendahl, "Electromagnetic fields (EMF): Do they play a role in children's environmental health (CEH)?" *Int. J. Hygiene Environ. Health*, vol. 210, pp. 635–644, Oct. 2007.

[23] A. A. Radzievsky, O. V. Gordiienko, S. Alekseev, I. Szabo, A. Cowan, and M. C. Ziskin, "Electromagnetic millimeter wave induced hypoalgesia: Frequency dependence and involvement of endogenous opioids," *Bioelectromagnetics*, vol. 29, no. 4, pp. 284–295, 2008.

[24] M. T. Jorge-Mora, M. Alvarez-Folgueiras, J. Leiro, F. J. Jorge-Barreiro, F. J. Ares-Pena, and E. López-Martín, "Exposure to 2.45 GHz microwave radiation provokes cerebral changes in induction of HSP-90 α/β heat shock protein in rat," *Prog. Electromagn. Res.*, vol. 100, pp. 351–379, 2010.

[25] M. T. Jorge-Mora, M. J. Misa-Agustiño, J. A. Rodríguez-González, F. J. Jorge-Barreiro, F. J. Ares-Pena, and E. López-Martín, "The effects of single and repeated exposure to 2.45 GHz radiofrequency fields on c-Fos protein expression in the paraventricular nucleus of rat hypothalamus," *Neurochem Res.*, vol. 36, no. 12, pp. 2322–2332, 2011.
[26] M. J. Misa-Agustiño, J. M. Leiro, M. T. J. Mora, J. A. Rodríguez-González, F. J. J. Barreiro, F. J. Ares-Pena, and E. López-Martín, "Electromagnetic fields at 2.45 GHz trigger changes in heat shock proteins 90 and 70 without altering apoptotic activity in rat thyroid gland," *Biol. Open*, vol. 1, no. 9, pp. 831–839, 2012.
[27] M. J. Misa-Agustiño, M. T. Jorge-Mora, F. J. Jorge-Barreiro, J. Suarez-Quintanilla, E. Moreno-Piquero, F. J. Ares-Pena, and E. López-Martín, "Exposure to non-ionizing radiation provokes changes in rat thyroid morphology and expression of HSP-90," *Exp. Biol. Med.*, vol. 240, no. 9, pp. 1123–1135, 2015.
[28] M. J. Misa-Agustiño, J. M. Leiro-Vidal, J. L. Gomez-Amoza, M. T. Jorge-Mora, F. J. Jorge-Barreiro, A. A. Salas-Sánchez, F. J. Ares-Pena, and E. López-Martín, "EMF radiation at 2450 MHz triggers changes in the morphology and expression of heat shock proteins and glucocorticoid receptors in rat thymus," *Life Sci.*, vol. 15, no. 127, pp. 1–11, 2015.
[29] A. López-Furelos, J. M. Leiro, J. A. Rodriguez-Gonzalez, M. M. Miñan-Maiques, F. J. Ares-Pena, and E. López-Martín, "An experimental multi-frequency system for studying dosimetry and acute effects on cell and nuclear morphology in rat tissues," *Prog. Electromagn. Res.*, vol. 129, pp. 541–558, 2012.
[30] A. López-Furelos, J. M. Leiro-Vidal, A. Á. Salas-Sánchez, F. J. Ares-Pena, and M. E. López Martín, "Evidence of cellular stress and caspase-3 resulting from a combined two-frequency signal in the cerebrum and cerebellum of Sprague-Dawley rats," *Oncotarget*, vol. 7, no. 40, pp. 64674–64689, 2017.
[31] J. L. Relova, S. Pértega, J. A. Vilar, E. López-Martín, M. Peleteiro, and F. Ares-Pena, "Effects of cell-phone radiation on the electroencephalographic spectra of epileptic patients," *IEEE Antennas Propag. Mag.*, vol. 52, no. 6, pp. 173–179, Dec. 2010.
[32] F. Vecchio, M. Tombini, P. Buffo, G. Assenza, G. Pellegrino, A. Benvenga, C. Babiloni, and P. M. Rossini, "Mobile phone emission increases inter-hemispheric functional coupling of electroencephalographic alpha rhythms in epileptic patients," *Int. J. Psychophysiol.*, vol. 84, no. 2, pp. 164–171, 2012.
[33] M. Tombini, G. Pellegrino, P. Pasqualetti, G. Assenza, A. Benvenga, E. Fabrizio, and P. Maria Rossini, "Mobile phone emissions modulate brain excitability in patients with focal epilepsy," *Brain Stimul.*, vol. 6, no. 3, pp. 448–454, 2013.
[34] G. Curcio, E. Mazzucchi, G. Della Marca, C. Vollono, and P. M. Rossini, "Electromagnetic fields and EEG spiking rate in patients with focal epilepsy," *Clin. Neurophysiol.*, vol. 126, no. 4, pp. 659–666, 2015.
[35] S. Mortavazi, A. Habib, A. Ganj-Karami, R. Samimi-Doost, A. Pour-Abedi, and A. Babaie, "Alterations in TSH and thyroid hormones following mobile phone use," *Oman Med. J.*, vol. 24, no. 4, pp. 274–278, 2009.
[36] M. Carlberg, L. Hedendahl, M. Ahonen, T. Koppel, and L. Hardell, "Increasing incidence of thyroid cancer in the Nordic countries with main focus on Swedish data," *BMC Cancer*, vol. 16, no. 1, p. 426, 2016. doi: 10.1186/s12885-016-2429-4.
[37] S. Thomas, A. Kühnlein, S. Heinrich, G. Praml, D. Nowak, R. von Kries, and K. Radon, "Personal exposure to mobile phone frequencies and well-being in adults: A cross-sectional study based on dosimetry," *Bioelectromagnetics*, vol. 29, pp. 463–470, 2008.
[38] S. Cakmak, R. E. Dales, and C. B. Vidal, "Air pollution and hospitalization for epilepsy in Chile," *Environ. Int.*, vol. 36, no. 6, pp. 501–505, 2010.
[39] L. Fajersztajn, M. Veras, L. V. Barrozo, and P. Saldiva, "Air pollution: A potentially modifiable risk factor for lung cancer," *Nature Rev. Cancer*, vol. 13, pp. 674–678, Sep. 2012.
[40] J. Emmerechts and M. F. Hoylaerts, "The effect of air pollution on haemostasis," *Hämostaseologie*, vol. 32, no. 1, pp. 5–13, 2013.
[41] J. Y. Ljubimova, O. Braubach, R. Patil, A. Chiechi, J. Tang, A. Galstyan, E. S. Shatalova, M. T. Kleinman, K. L. Black, and E. Holler, "Coarse particulate matter (PM 2.5–10) in Los Angeles Basin air induces expression of inflammation and cancer biomarkers in rat brains," *Sci. Rep.*, vol. 8, Apr. 2018, Art. no. 5708.
[42] P. R. Doyon and O. Johansson, "Electromagnetic fields may act via calcineurin inhibition to suppress immunity, thereby increasing risk for opportunistic infection: Conceivable mechanisms of action," *Med. Hypotheses*, vol. 106, pp. 71–87, Sep. 2017.
[43] T. Ku, X. Ji, Y. Zhang, G. Li, and N. Sang, "$PM_{2.5}$, SO_2 and NO_2 co-exposure impairs neurobehavior and induces mitochondrial injuries in the mouse brain," *Chemosphere*, vol. 163, pp. 27–34, Nov. 2016.
[44] Q. Zhang, Q. Li, J. Ma, and Y. Zhao, "$PM_{2.5}$ impairs neurobehavior by oxidative stress and myelin sheaths injury of brain in the rat," *Environ. Pollut.*, vol. 242, pp. 994–1001, Nov. 2018.
[45] R. N. Kostoff and C. G. Y. Lau, "Combined biological and health effects of electromagnetic fields and other agents in the published literature," *Technol. Forecast. Soc. Change*, vol. 80, no. 7, pp. 1331–1349, 2013.
[46] T. L. Watterson, B. Hamilton, R. Martin, and R. A. Coulombe, Jr., "Urban particulate matter causes ER stress and the unfolded protein response in human lung cells," *Toxicol. Sci.*, vol. 112, no. 1, pp. 111–122, 2009.

AARON A. SALAS-SÁNCHEZ was born in A Coruña, Spain, in 1988. He received the bachelor's degree in physics, the M.S. degree in engineering mathematics, and the Ph.D. degree in mathematical modelling and numerical simulation in engineering and applied science, in 2012, 2014, and 2018, respectively, from the University of Santiago de Compostela, Spain. He was Visiting Ph.D. Student with the Department of Electrical Engineering and Information Technology, University Federico II of Naples, Italy, in 2015. He is currently a Xunta de Galicia International Postdoctoral Fellow (ref. ED481B 2018/008) with the Department of Applied Physics, University of Santiago de Compostela, which brings him the opportunity to be Visiting Postdoctoral Researcher with ELEDIA Research Center, University of Trento, Italy, by two years. He serves as a Reviewer for different international journals including the IEEE TRANSACTIONS ON ANTENNAS AND PROPAGATION, THE IEEE ANTENNAS AND WIRELESS PROPAGATION LETTERS, and IET Microwaves, Antennas and Propagation. His current research interests include numerical methods in solving electromagnetic problems and antenna array pattern synthesis.

ALBERTO LÓPEZ-FURELOS was born in Santiago de Compostela, Spain, in 1987. He received the B.S. degree in biology, the M.S. degree in biotechnology, and the Ph.D. degree in medicine in 2010, 2012, and 2018, respectively, from the University of Santiago de Compostela, Spain.

His current research interest includes biological effects of non-ionizing radiation.

J. ANTONIO RODRíGUEZ-GONZÁLEZ (M'01–SM'05) was born in Orense, Spain, in 1972. He received the B.S. and M.S. degrees in physics, and the Ph.D. degree from the University of Santiago de Compostela, Spain, in 1995, 1996, and 1999, respectively.

He is currently an Associate Professor with the Department of Applied Physics, University of Santiago de Compostela. He has authored more than 200 papers for journals, conferences, and collaborative volumes. His research interests include numerical methods for solving electromagnetic problems and pattern synthesis, computer programming, and software engineering.

Dr. Rodriguez Gonzalez was the Secretary of the Spanish Committee of the International Union of Radio Science (URSI), from 2011 to 2017. He received the Outstanding Ph.D. Award from Physics Faculty, University of Santiago de Compostela, in 2000, and was awarded the teaching innovation prize at the University of Santiago de Compostela, in 2006.

FRANCISCO J. ARES-PENA (M'94–SM'96–F'09) received the B.S., M.S., and Ph.D. degrees in physics from the University of Santiago de Compostela, Spain, in 1986, 1987, and 1993, respectively.

He was a Research Scholar with the Department of Electrical Engineering, University of California, Los Angeles, for two quarters, in 1990 and 1991, where he developed the main topic of his Ph.D. thesis. He is currently Full Professor with the Department of Applied Physics, University of Santiago de Compostela, Spain. He has authored more than 380 papers for journals, conferences and collaborative volumes. His current research interests include numerical methods in solving electromagnetic problems and antenna array pattern synthesis.

Prof. Ares-Pena serves as an Associate Editor of the IEEE TRANSACTIONS ON ANTENNAS AND PROPAGATION. He received the Outstanding Ph.D. Award from the Physics Faculty, University of Santiago de Compostela, in 1994, and awarded the teaching innovation prize of the University of Santiago de Compostela, in 2006. He was also a President of the Spanish Committee of the International Union of Radio Science (URSI), from 2011 to 2017.

M. ELENA LÓPEZ-MARTíN was born in Segovia, Spain, in 1963. She received the Ph.D. in medicine from the University of Santiago de Compostela, Spain, in 1999.

She is currently an Associate Professor of human anatomy with the Morphological Sciences Department, University of Santiago de Compostela.

Dr. López-Martín has authored or coauthored more than 104 papers and scientific communications. Her current research interests include the study of electromagnetic pollution, the biological effects of mobile telephony and the therapeutic application of microwaves in the central nervous system (CNS) and peripheral tissues. Since 2013, she has been the Spanish Official Member of the Commission K (Electromagnetics in Biology and Medicine) in the International Union of Radio Science (URSI). She serves as a reviewer for different international journals, including the *Progress in Electromagnetic Research* (PIER), *Bioelectromagnetics*, *Biomedical and Environmental Science*, *Mutation Research*, and the *International Journal of Radiation Biology*.